

Highly siderophile element abundances and ^{187}Re - ^{187}Os
isotope systematics of Gorgona Island komatiites and
Costa Rican picrites

Kyle Ludwig

Advisors: Dr. Richard J. Walker, Dr. Igor Puchtel, Dr. Katherine R. Bermingham
Department of Geology, University of Maryland, College Park, MD, 20740

GEOL 394 - Final

April 19, 2017

Abstract

New Re-Os isotope and highly siderophile element (HSE) data are reported for a komatiitic lava flow on the east coast Gorgona Island, two komatiites from the western side of the island, and for three picrites from the Tortugal Suite of Costa Rica. The Gorgona Island komatiites are among the youngest in the world (89.2 ± 5.2 Ma), with the picrites being similar in age (~ 89 Ma). It has been reported that these suites were formed from melts originating at high mantle temperatures ($>1500^\circ\text{C}$) from a mantle plume. This plume hypothesis has been widely accepted as the source for Large Igneous Provinces (LIP) in general, and in this case, the Caribbean Large Igneous Province (CLIP). Temperatures in portions of this plume reach Archean levels, which could cause the high degree melts at great depth to form komatiitic lava.

This study reports Re-Os and HSE data that indicate large-scale heterogeneity of the CLIP plume. The east coast Gorgona komatiites represented in this study have γOs (deviation from chondritic) values ranging from +0.2 to +2.0, whereas the Tortugal picrites have γOs values ranging from -2.8 to -1.6 and west coast komatiites between +10.6 and +13.1. These results suggest that the eastern komatiite flow examined in this study is slightly enriched, and is likely a slightly open system. The western komatiites, however, are much more enriched in Re, and were sourced from an isotopically enriched portion of the plume. In addition, the Tortugal suite was sourced from a depleted Re mantle source, and therefore also represents a different part of the CLIP.

1. Introduction

It is generally accepted that the Caribbean Large Igneous Province (CLIP) originated from a mantle plume (Trela et al. 2017; Walker et al. 1999; Arndt et al. 1997; Alvarado et al. 1997). This study examines the heterogeneity of the CLIP mantle plume through use of highly siderophile element systematics and the rhenium osmium isotope system. Rhenium - osmium is an important system because of its unique chemical characteristics. Both elements are siderophile, but also have chalcophile tendencies and therefore they differ largely from many of the other common radiogenic isotope systems (many of which are lithophile) such as Sm-Nd and Lu-Hf. It is this siderophile tendency that causes them to concentrate in the earth's core and have low concentrations in the mantle and especially the crust. The Gorgona komatiites and Tortugal picrites are prime candidates for Re and Os isotopic variations due to their young age, (89.2 ± 5.2 Ma), their ultramafic parental liquids had high Os concentrations, and the rocks that crystallized from these liquids have (relatively) low Re/Os ratios. The young age of these rocks is helpful for the assessment of the GOR 152 – 160 flow for open or closed system behavior, as there has been little time since crystallization for alteration. Open system behavior has been suggested in previous studies as a model for enrichment in Re in the komatiites, but none of these studies have analyzed the GOR 152 – 160 flow or the Tortugal picrites for Re/Os systematics (Echeverria et al. 1986; Walker et al. 1999). This system along with the study of other highly siderophile element (HSE; including Re, Os, Ir, Ru, Pt, and Pd) fractionation can offer insight into chemical and isotopic heterogeneity in the CLIP plume, as well as within the flows themselves.

Prior studies have reported highly variable initial osmium isotopic compositions for the ultramafic suite of Gorgona, which was interpreted as indicating isotopic heterogeneity in the mantle source (Walker et al., 1991; Walker et al., 1999; Brandon et al., 2003). γOs for Gorgona komatiites range from -0.5 to +12.4 (Walker et al., 1999), where γOs is the percent deviation of

the $^{187}\text{Os}/^{188}\text{Os}$ ratio of a sample from chondrite osmium evolution at the time of formation. Large variations in major and trace element compositions throughout this suite have also been reported for komatiites on the island, as well as several possible mechanisms to explain these compositional variations. These explanations include olivine fractionation (Echeverria et al., 1980), mantle source heterogeneity (Walker et al., 1991; Walker et al., 1999), and dynamic melting in a depleted mantle plume (Arndt et al., 1997).

2. Hypotheses

The Gorgona 152-160 komatiite flow represents a lava flow from the eastern side of the island, and because they are from a sole source it is expected that these samples will have the same initial $^{187}\text{Os}/^{188}\text{Os}$ ratios, and if they have experienced little or no outside Re loss, the flow will exhibit closed system behavior. This behavior would require that the ratios for all samples within the flow plot on or within the margin of error of an 89 Ma Re-Os reference isochron. The 152 – 160 flow is also expected to fractionate HSE preferentially as an olivine controlled system due to the layering and fractionation that is seen in komatiite flows. (Puchtel et al. 2009; Puchtel et al. 2016).

On the western side of the island, however, it is expected that the western komatiite samples (23B and 47) will represent a more enriched $^{187}\text{Os}/^{188}\text{Os}$ source, which causes them to fall far above the 89 Ma isochron. Previous studies have reported high Re isotopic ratios from that side of the island (Walker et al. 1999), and it is expected that the results of this study will be similar. These high $^{187}\text{Os}/^{188}\text{Os}$ could also be a result of open system behavior, but it seems very unlikely due to the shear amount of Re that would have to leave the system to explain the reported ratios from Walker et al. (1999). It is expected that this study will confirm the prior hypothesis that these ratios are representative of a portion of the mantle source for these rocks.

The suite of Costa Rican picrites from the ultramafic Tortugal suite are connected to the Gorgona komatiites because they are both associated with the CLIP (Trela et al. 2015; Trela et al. 2017). The similar lithologies and formation times of the region, mean that they should have the same source in the plume that created the CLIP, and it is expected that they have similar initial $^{187}\text{Os}/^{188}\text{Os}$ ratios to the Gorgona suite. They should also have similar Re-Os systematics because of their being from the same reservoir.

The HSE concentrations of the GOR 152 - 160 komatiite flow are expected to behave in a manner consistent with olivine fractionation throughout the flow. This would be evident through negative incompatible HSE trends (Pt, Rd, and Re). These trends, considered “olivine control lines” would be negative due to the decreased incompatible HSE concentrations as the olivine content (and as a result, the MgO content) increases (Puchtel et al. 2005; Puchtel et al. 2009).

3. Geology

3.1 – Gorgona Island

Gorgona Island is a small Island approximately 8 km long and 2.5 km wide located 50km off the Pacific coast of Colombia (Fig. 1). The geology was first described in detail by Gansser (1950), Gansser et al. (1979), and Echeverria (1980). The island is covered by a dense rain forest, and features various geomorphic features such as vertical cliffs, steep slopes, and an absence of terraces – all of which attest to the young age of the island and possible continued

uplift. The geology has been described as a sequence of uplifted and tilted mafic and ultramafic rocks (Echeverria et al., 1980). The island represents part of the Serrania de Baudo, which is the

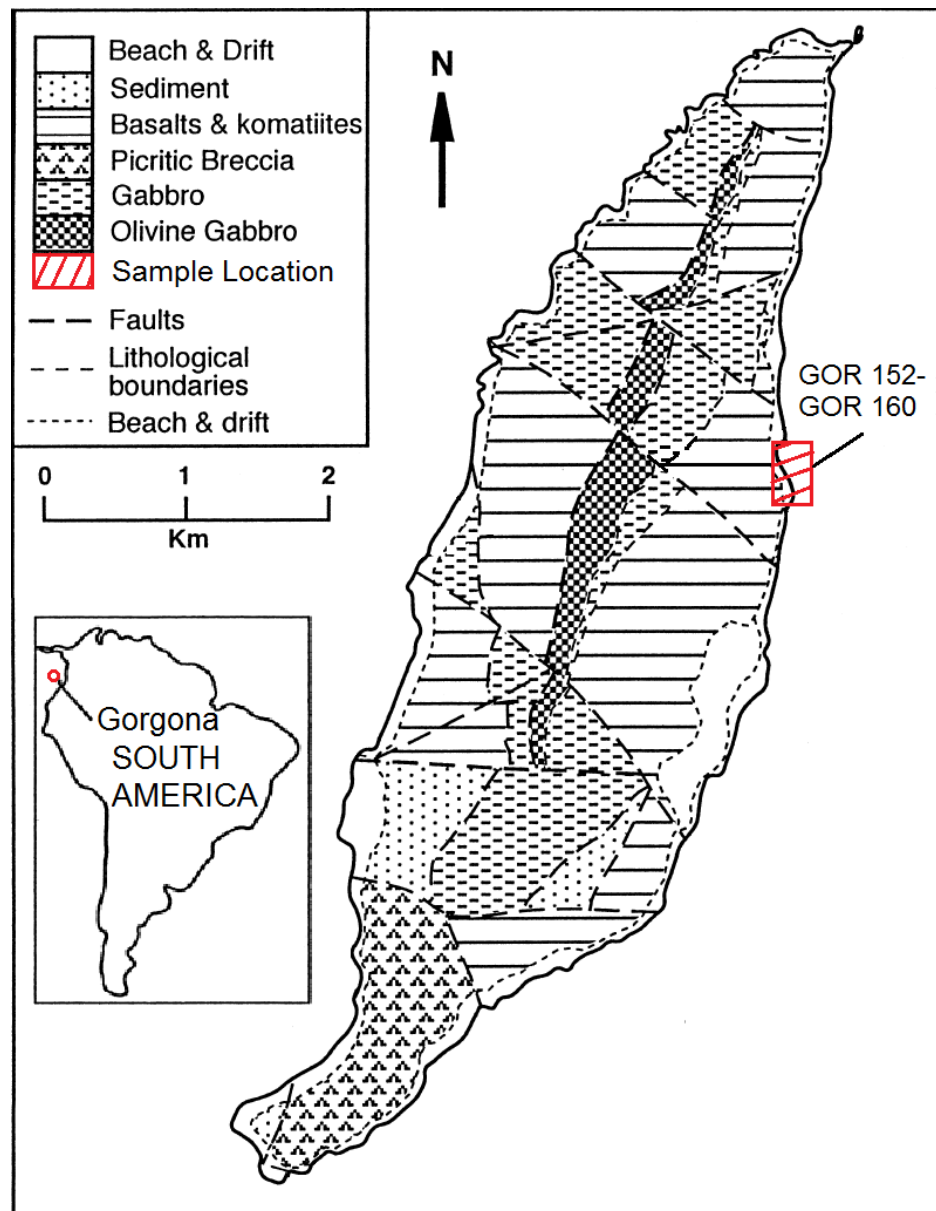


Fig. 1. Map of Gorgona Island geology and sample location. Modified from Walker et al., (1999)

youngest igneous and sedimentary belt on the western margin of Colombia that accreted during the late Cretaceous and early Tertiary (Kerr et al., 1996). Re-Os and Pb-Pb data indicate a crystallization age of the ultramafic suite on the island of ~89.2 Ma (Walker et al., 1999). Most komatiites formed during the Archean Eon (Arndt et al., 2008), so these 89 Ma rocks are the youngest komatiites recorded.

3.2 - Komatiite Flow

Studying primary melts from mantle plume derived lavas can offer insight to the mantle melting conditions during formation (Trela et al. 2017). When the mantle melts at high temperatures ($>1500^{\circ}$), it can produce an ultramafic lava, which forms by extensive melting of source, or melting of a source that is very refractory (Arndt et al. 2003). They are distinguished as ultramafic, high temperature, and magnesium-oxide (MgO) rich rocks that usually exhibit a unique quenched spinifex texture (Gansser et al., 1979; Arndt et al., 1980; Arndt et al., 2008). The spinifex zone represents the majority of the GOR 152 – 160 flow, and exhibits poorly formed crisscrossing olivine spinifex with a pyroxene and glass matrix (Figs. 9 - 13). Because this flow is weakly differentiated, there is no peridotite cumulate zone. This can be explained by the low levels of MgO across the flow. A cumulate zone is generally seen as having $>30\%$ MgO (Arndt et al, 1980). This fractionation is caused by the olivine falling out of suspension in the liquid during crystallization. It is likely most komatiites formed due to high degrees of anhydrous partial melting of the mantle during ascent (Arndt et al. 2008). High degrees of mantle melting can result in the extraction of a large portion of HSE, leading to the partitioning of those HSE into komatiites from their mantle sources (Barnes et al. 1985; Puchtel et al., 2009). These HSE signatures can be characteristic of emplacement and classifications of different komatiites. For example, negative trends in incompatible HSE (Pt, Pd, and Re) always plot on negative trends in komatiites with olivine control (Puchtel et al. 2009).

Komatiites generally form flows that are differentiated with respect to texture, mineral composition, and bulk rock composition. For example, the upper portions of komatiite flows are generally more Al_2O_3 , CaO, and Na_2O rich as compared to the lower cumulate zone (Arndt et al. 1980). Archean Komatiite flows are typically described in three zones: an upper chilled and fractured margin, a spinifex zone, and a lower cumulate zone (Pyke et al. 1973; Arndt et al. 1977). The upper chilled margin is a representation of the emplaced lava, and is first of the lava flow to crystallize. The GOR 152- 160 reported in this study differs from typical Archean differentiated komatiite lava flows in that it does not have a lower cumulate zone. There is however, still a distinct fractionation of MgO throughout the layers of the flow. This change in MgO content as a function of depth in the flow is a result of preferential crystallization olivine in the flow, and a sign that olivine is the major phase in the rocks.

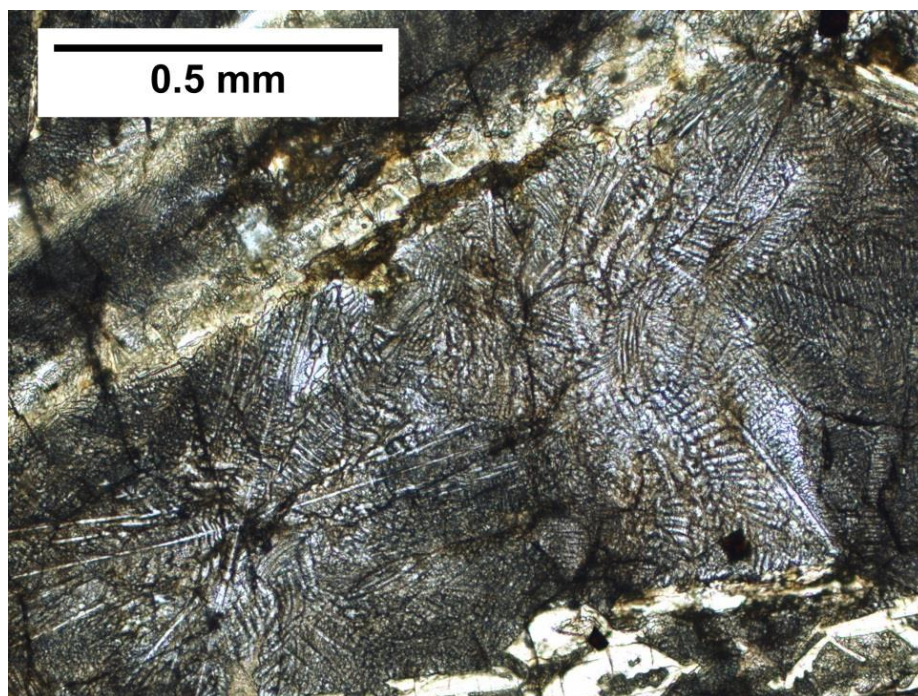


Fig. 2. Photomicrograph of skeletal clinopyroxene texture in upper chill margin komatiite (GOR 152). Larger olivine crystals can be seen at the bottom right of the image (white in PPL) Image is 1.4mm across and is in plane polarized light.

4. Analytical Techniques

4.1 – Sample Preparation

The samples were collected by Echeverria (1980), and are currently housed at the Smithsonian Institution National Museum of Natural History (NMHN). The samples were provided in whole rock form. The komatiites samples were prepared using standard methods (Puchtel et al., 2016; Puchtel et al., 2009). The rocks (ranging from 50 to 300 g) were broken into 2 – 3 cm pieces using anvil and hammer, with both wrapped in polyvinyl chloride plastic to avoid metal contamination. Possible contamination due to weathering was removed prior to crushing using SiC sandpaper. These pieces were then crushed in an alumina-faced jaw crusher to <5 mm grains. A 20 to 50 g aliquot of each sample was then ground in an alumina-faced shatter box (cleaned with quartz sand between each sample), followed by a fine re-grinding using an alumina-faced disk mill.

4.2 – Major, minor, and trace elements

Major elements were commercially analyzed at Franklin and Marshall College using fusion glass disks with a Phillips 2404 X-ray fluorescence (XRF) vacuum spectrometer. The techniques are detailed in Mertzmann (2000). Cited precision is ~1% (2SD) for most major elements (>0.5 wt%), and between 1-5% (2SD) for elements with abundances <0.5% (Mertzmann (2000); Puchtel et al., 2016). Major element data are reported in Appendix I.

4.3 – Os Isotope Data

4.3.1 - Digestion

In order to separate osmium and other HSE elements from the bulk rock, samples are digested and osmium is isolated and purified using methods described in Puchtel et al. (2016). In short, appropriate amounts of concentrated HCl and spike which include various abundances of ^{99}Ru , ^{105}Pd , ^{190}Os , ^{191}Ir , ^{194}Pt , and ^{195}Re , were added in a clean environment to approximately 1 g of each powder. The spike is a mixture of known PGE abundances that increases the amount of each element in the sample to ease the measurement. The known spike is then subtracted out of the analysis at the end. This solution is added to an internally cleaned (via aqua regia) Pyrex Carius tube. At this point we add concentrated HNO_3 to create aqua regia in the powder and spike solution. The tube is subsequently sealed with an oxy-propane torch, placed in metal jackets (to protect the other tubes in the event of an explosion), and heated to a temperature of approximately 270°C . The tube is later broken open and the mixture of sample, spike, and aqua regia is then added to a 60ml centrifuge tube and mixed with 3mL of carbon tetrachloride. This mixture is centrifuged to separate the liquid phases by density. The denser carbon tetrachloride mixture is then pipetted out and added to a Teflon beaker containing 4mL of HBr (hydrobromic acid). This process of adding carbon tetrachloride, centrifuging, and removing is repeated 2 more times (adding more carbon tetrachloride and centrifuging each time). The centrifuge tube is then set aside for the later HSE chromatography. The Teflon beaker is then heated on a hot plate and the denser carbon tetrachloride is disposed of (All osmium will have transferred to the HBr). Finally, the aqua regia is then dried down to a small drop ($\sim 40\ \mu\text{L}$).

4.3.2 – Micro Distillation

This drop is now put on the cap of a 5mL conical bottom Teflon vessel and is evaporated until dry. Fifteen μL of HBr is then added to the bottom of the 5mL Teflon, and 20-30 μL of dichromate solution is added to the dried down spot of sample on the cap. The vessel is then closed and put on a hot plate at 85°C inverted for 2-3 hours (keeping the HBr suspended in the conical bottom). Milli-Q water is then added to the cap to check for osmium oxidation. If the dichromate solution turns yellow, there has been sufficient Cr^{+6} to oxidize the osmium, and the HBr solution can be fully dried under a heat lamp.

4.3.3 – Thermal Ionization Mass Spectrometry

The separated osmium was then placed on degassed Pt filaments and loaded into a negative thermal ionization mass spectrometer (TIMS). All samples were analyzed using a secondary electron multiplier (SEM) on a ThermoFisher TritonTM mass spectrometer at the Isotope Geochemistry Laboratory (IGL), University of Maryland. The mass fractionation correction ratio of $^{190}\text{Os}/^{188}\text{Os}$ used was 3.0832. Precision for all $^{187}\text{Os}/^{188}\text{Os}$ samples is between 0.03 – 0.1% relative (2 standard-errors). All TIMS data are reported in Table 1, and are reported as $^{187}\text{Os}/^{188}\text{Os}$ ratios. These ratios were then used to calculate Re/Os ratios, Os concentrations, initial $^{187}\text{Os}/^{188}\text{Os}$ ratios, and γOs .

4.4 – Highly Siderophile Elements

4.4.1 – Chromatography

The aqua regia solution from the centrifuge tube set aside during Os separation is now pipetted into a Teflon beaker and is dried down under a heat lamp. In order to purify the solution, 2 rounds of 2.5 to 10ml of 1 N TD HCl (1 normal Teflon distilled) is added to the semi solid, and is dried under a heat lamp. This process removes the last of the aqua regia from solution. Each sample then goes through a various rounds of different acids in order to separate Re+Ru, Pt+Ir, and Pd into separate Teflon beakers. The Re and Ru then go through a secondary elution column for further cleaning with various stages of acids and water. After these final cleaning procedures, the samples are ready for the ICP-MS.

4.4.2 – Inductively Coupled Plasma Mass Spectrometry

Measurements for Ir, Ru, Pt, Rd, and Re were performed in the University of Maryland Plasma Laboratory using a Nu Plasma™ multi collector inductively coupled plasma mass spectrometer (MC-ICP-MS) with a triple electron multiplier configuration in static mode. Blank calculations for each of the HSE are as follows: palladium: 17.3 pg, platinum: 340 pg, ruthenium: 6.8 pg, and iridium: 0.28 pg.

5. Results

5.1 – Gorgona Island Komatiite Flow

This flow had relatively low Re and Os concentrations. All whole rock Re and Os concentrations for the GOR 152 – 160 flow fell between 0.451 to 1.06ppb and 1.371 to 3.592 ppb, respectively. The $^{187}\text{Re}/^{188}\text{Os}$ ratios for the flow between 0.875 and 2.868 and are reported in Table 1. Samples are plotted with an 89 Ma reference isochron along with previous Re-Os data from previous studies from both sides of the island. (Walker et al. 1999; Fig 10). The samples from this flow plot slightly above the reference isochron, with very close together γOs ranging from +0.2 to +2.0. γOs represents the percent deviation of $^{187}\text{Os}/^{188}\text{Os}$ in the sample from the chondritic value of $^{187}\text{Os}/^{188}\text{Os}$ at a specific time (Walker et al., 1989).

$$\frac{\left(\frac{^{187}\text{Os}}{^{188}\text{Os}}\right)_t(\text{Sample}) - \left(\frac{^{187}\text{Os}}{^{188}\text{Os}}\right)_t(\text{Chondritic})}{\left(\frac{^{187}\text{Os}}{^{188}\text{Os}}\right)_t(\text{Chondritic})} * 100 = \gamma\text{Os}$$

Equation 1. γOs represents the percent deviation from chondritic values of osmium from a specific time (of formation). In the case of this study, the initial time of formation is 89Ma.

Walker et al. (1999) reported γOs for the eastern komatiites between +0.9 and +2.7 (excluding one sample). These values are very similar to the GOR 152 – 160 flow, and are all very close to chondritic. Initial $^{187}\text{Os}/^{188}\text{Os}$ values for the flow are all very consistent, ranging from 0.1266 to 0.1289 (Table 1), and support long-term chondritic values of γOs .

The GOR 152- 160 flow exhibits olivine controlled fractionation of MgO as indicated by the negative correlations between MgO and the incompatible HSE (Pt, Pd, and Re) (Fig. 4). There is no such strong correlation in the MgO vs. Os, Ir, or Ru plots. The HSE are also plotted on a chondrite normalized plot (Fig. 5) that illustrates the deviation from chondritic throughout the flow.

Repetition analysis was done for both Os analysis via TIMS and HSE analysis via ICP-MS on a sample of the GOR 152 – 160 flow (GOR 159). The uncertainties for this study were assessed by 2 standard deviation of the difference between these two analyses. The error between replicated samples was the largest when compared to counting errors and instrument errors, and is therefore the most reliable error value. Errors for the HSE analysis range from 0.7% to 7.5% (according to the reproducibility). Errors in $^{187}\text{Re}/^{188}\text{Os}$ range from ~1% to 1.8% for the eastern komatiite flow and the Tortugal picrites, and ~2.5% to 3% for the Western komatiites. $^{187}\text{Os}/^{188}\text{Os}$ error is between ~0.06% and 0.2% for all samples.

Table 1. Rhenium and Os isotopic and compositional data for Gorgona island and the Costa Rican picrites.

Sample	Lithology	MgO	Os	Re	$^{187}\text{Os}/^{188}\text{Os}$	$^{187}\text{Re}/^{188}\text{Os}$	$^{187}\text{Os}/^{188}\text{Os}(t)$	γOs
<i>Gorgona Island, East</i>								
GOR 152	komatiite	15.33	2.417	0.859	0.1308	1.713	0.1282	+1.5
GOR 153	komatiite	23.8	1.371	0.816	0.1319	2.868	0.1273	+1.0
GOR 155	komatiite	15.45	2.485	0.451	0.1302	0.875	0.1289	+2.0
GOR 156	komatiite	17.65	2.672	1.060	0.1303	1.912	0.1275	+0.9
GOR 157	komatiite	12.14	3.064	0.965	0.1299	1.517	0.1277	+1.0
GOR 159	komatiite	18.77	3.592	0.883	0.1296	1.184	0.1279	+1.1
Replicate			3.304	1.028	0.1297	1.499	0.1275	+0.9
GOR 160	komatiite	17.76	3.331	0.948	0.1286	1.371	0.1266	+0.2
<i>Gorgona Island, West</i>								
GOR23B	komatiite	18	0.785	1.187	0.1507	7.3063	0.1398	+10.6
GOR47	komatiite	17.6	0.813	0.802	0.1500	4.7667	0.1430	+13.1
GOR 23A	basalt	5.25	0.091	0.779	0.2077	41.8880	0.1455	+15.1
<i>Tortugal Suite</i>								
TO-010513-5	picrite	30.58	5.123	0.021	0.1240	0.0168	0.1240	-1.9
TO-080514-2	picrite	32.22	6.270	0.054	0.1229	0.0391	0.1228	-2.8
TO-080614-5	picrite	31.45	3.988	0.053	0.1245	0.0600	0.1244	-1.6

Rhenium and Os concentrations in ppb. MgO concentrations in wt%. γOs values are calculating assuming an age of 89 Ma for both Gorgona and Costa Rica with a chondritic $^{187}\text{Os}/^{188}\text{Os}$ value at the time of 0.12653 using a λ for $^{187}\text{Re} = 1.666 \times 10^{-11} \text{a}^{-1}$ (Walker et al. 1999)

5.2 – West Coast Komatiites

Two western komatiites were analyzed so help assess open or closed system behavior of the GOR 152 – 160 flow. These two samples (GOR 23B and GOR 47) have Re-Os isotope data (Walker et al. 1999), and have been examined again to further backup what was reported in Walker et al. (1999). These samples were previously found to have some of the highest γ_{Os} of any komatiites on the island (+11.1 to +12.4). These γ_{Os} values are similar to those reported in this study (+10.6 to +13.1) with an error of approximately 1.2% (error due to reproducibility of GOR 159). Within the margin of this error, the Re-Os ratios are consistent with each other. These samples plot high above the 89 Ma isochron (Fig. 3), but plot alongside other western komatiites.

5.3 – Costa Rican Tortugal Suite

Three samples from the Tortugal suite of picrites have been analyzed in a similar fashion as the Gorgona samples. HSE concentrations and Re-Os isotope systematics are reported in Table 1. These picrites have negative γ_{Os} values ranging from -1.6 to -2.8. This means that the value of Os in the sample today is lower than that of normalized chondritic values. Re-Os ratios for these samples are significantly lower than the Gorgona samples (ranging from 0.017 to 0.060). These low ratios plot the picrites significantly below the 89 Ma reference isochron. These samples also have significantly higher Os (3.98 – 6.27ppb) and MgO (30.6 – 32.2wt%). The HSE pattern for these rocks (Fig. 6) is significantly different than the pattern of the GOR 152 – 160 flow (Fig. 5). There is a significant enrichment in both compatible and incompatible HSE except Re.

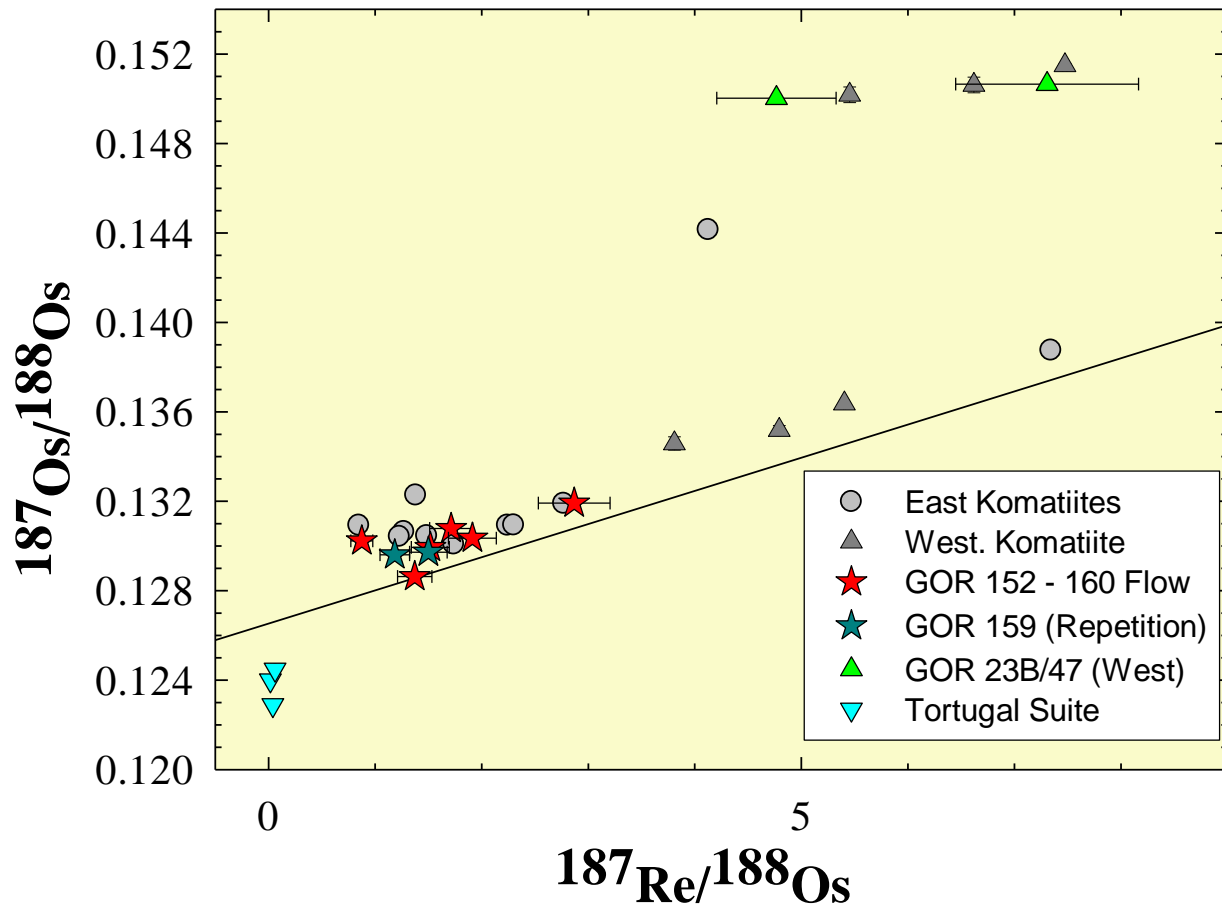


Fig. 3: This is a graph of $^{187}\text{Os}/^{188}\text{Os}$ vs $^{187}\text{Re}/^{188}\text{Os}$ with an 89 Ma chondritic reference isochron. “Eastern komatiites” and “western komatiites” (both in grey) represent data from Walker et al., (1999). Red stars denote the 152 – 160 flow and fall near or slightly above the isochron indicating a slight enrichment in Re. Dark red stars indicate the replication of GOR 159 Note western komatiite outliers above isochron with the GOR 23B/47 repetition falling very close. Figure adapted from Walker et al., (1999).

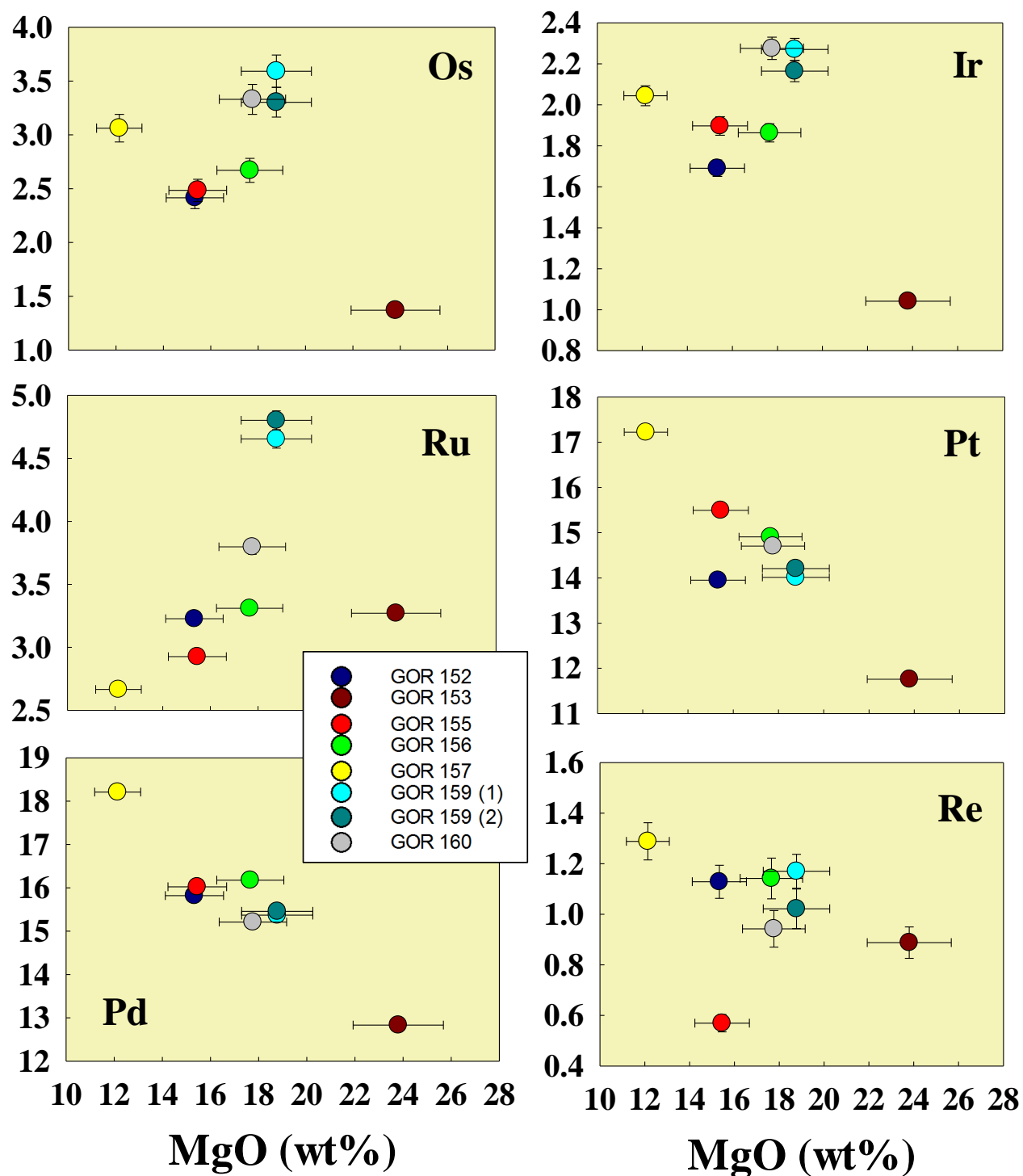


Fig 4: HSE concentrations vs. MgO of the GOR 152 – 160 flow. All y axis (differing HSE) values are in ppb, and x axis (MgO) values are in wt%. Note the negative trends in Pt, Pd, and Re which create negative olivine control lines

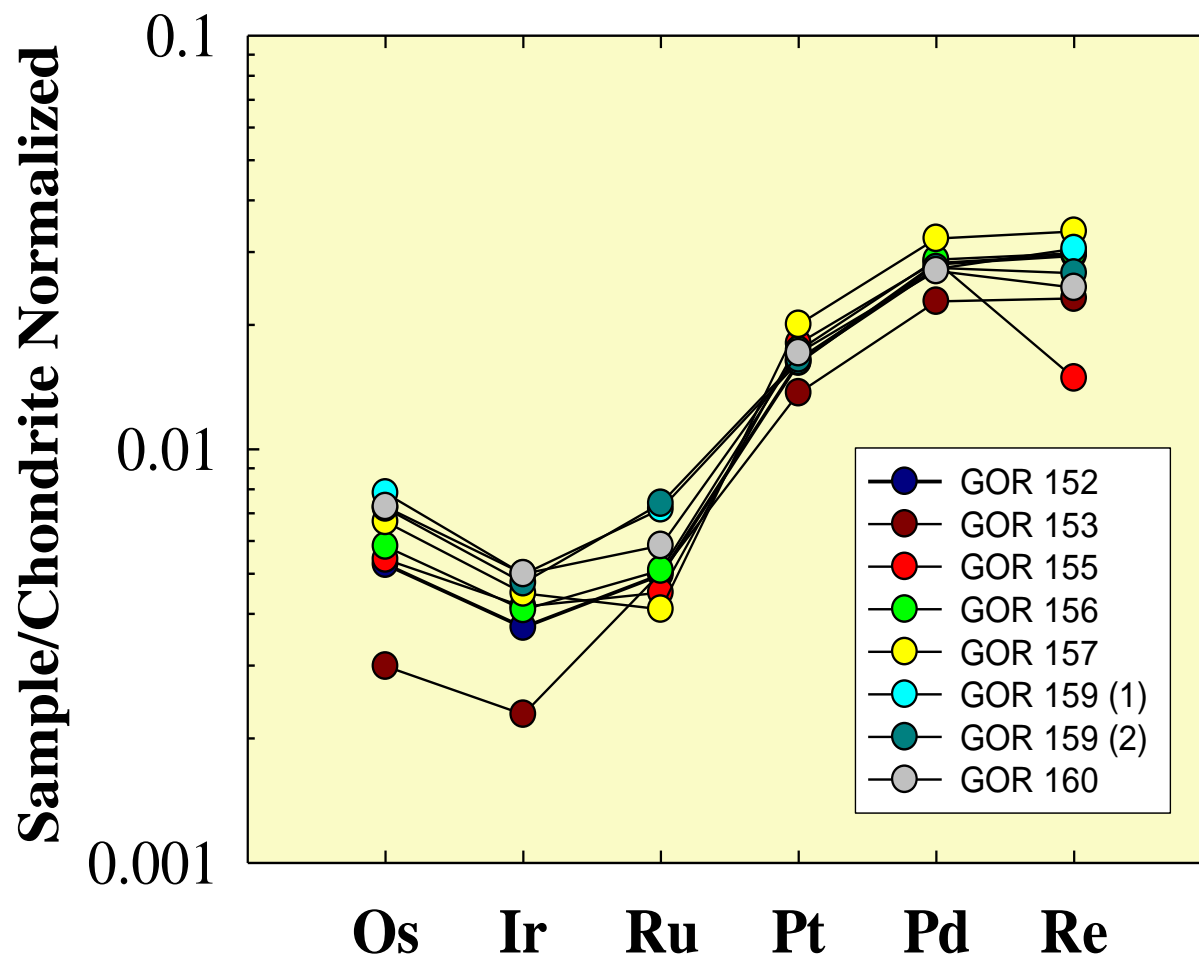


Fig. 5: HSE patterns for the GOR 152 – 160 flow of komatiites. Note the high enrichment of Pt, Pd, and Re throughout the flow, and the general trend of enrichment as the flow progresses through the upper chilled margin to the spinifex zone.

6. Discussion

Past studies have found significant differences in Os, Ir, Ru, Pt, Pd, and Re isotopic compositions within the Caribbean LIP. There have been two hypothesized possibilities published to explain the apparent variability of these elements within the CLIP. The first explanation is that the more radiogenic compositions represent different mantle sources or portions of the plume being sourced to form different outcrops within the CLIP. The second proposed explanation is that the samples that deviate from chondritic exhibit open-system behavior after crystallization (Walker et al. 1999).

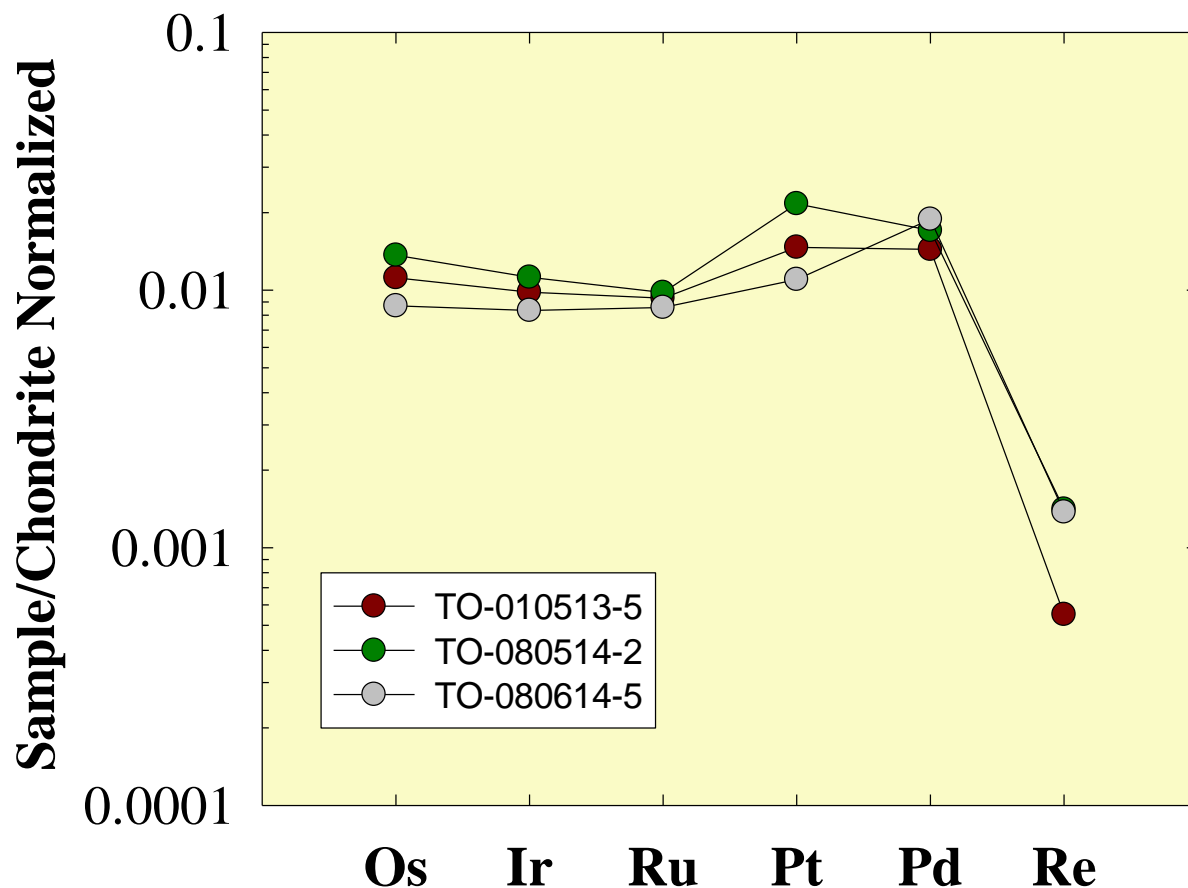


Fig. 6: This graph is the HSE pattern for the Tortugal suite of picrites. Note the high depletion of Re.

The samples of the GOR 152 -160 flow plot close together near other eastern komatiites, all on (or slightly above) the 89 Ma reference isochron (Fig. 3). In order for these samples to be a fully closed system as was originally hypothesized, they would all have to plot on the isochron, or be within the range of uncertainty. However, because all of the samples do not plot of this isochron, there must be some small aspect of open system within this flow. The samples do however have very similar $^{187}\text{Os}/^{188}\text{Os}$ initial values (0.1266 to 0.1289) to the assumed chondritic $^{187}\text{Os}/^{188}\text{Os}$ ratio at 89 Ma (0.12653) (Walker et al. 1999). Through this would be expected if because they appear to be sourced from a chondritic source within the CLIP plume.

The western komatiites differ greatly from the eastern GOR 152 – 160 flow. Walker et al. (1999) suggested that open system behavior was not a sufficient means of explaining the isotopic heterogeneity of the western komatiites compared to the eastern. These 2 komatiites plot well above the 89 Ma isochron (Fig. 3). The explanation that a >50% reduction in Re we see reported in the western komatiites is just a consequence of open system behavior is too unlikely to support, especially considering the widespread heterogeneity of this plume. With that in mind, the findings in this study confirm the prior hypothesis that the ratios are representative of portion

of the mantle source for these rocks is different than the source for the eastern komatiites, though they are both part of the CLIP.

The HSE patterns for the GOR 152 – 160 flow indicate a strong negative trend for Pt, Pd, and Re as was stated above. This negative trend is a result of incompatible HSE not crystalizing in olivine. Because of this, an olivine controlled system will have lower incompatible HSE the higher the olivine (or MgO in this case) content gets because Olivine is the only major phase that is accepting these HSE. As can be seen in Fig. 4, the strong negative trend in MgO vs. Pt, Pd, and Re must indicate an olivine controlled system, which was expected due to the large MgO content of these rocks, and their preferential crystallization of olivine.

The HSE patterns of the eastern komatiite flow can be weakly defined as a Munro-type komatiite due to the slightly positive compatible HSE slopes (Os, Ir, Ru) (Puchtel et al. 2005). Although this classification is generally applied to Archean komatiites, there is a slight trend in these three HSE. The positive trend is a result of not only olivine, but Os and Ir alloys. In order to fully address this issue of classification, however, the alloys and olivine mineral separates must also be analyzed.

The Tortugal suite is part of the CLIP, so it would be expected that the samples from the suite would have similar Re-Os isotopic ratios as was hypothesized, however, they do not. The 3 samples plot very close together on the isochron plot (Fig. 10), indicating a homogeneity within that suite, but the lava as a whole is slightly depleted in Re with negative γ_{Os} values. These samples (similar to the western komatiites) must represent a different source region from the plume. Although formed at similar times, the initial $^{187}Os/^{188}Os$ for these samples is significantly lower (0.1229 to 0.1245). Although these rocks originated from the sample CLIP as the Gorgona komatiites, the isotope data shows that these samples must have formed from another section of the plume.

Acknowledgments

Thank you to my advisors, Dr. Richard Walker, Dr. Igor Puchtel, and Dr. Katherine Bermingham for all of their guidance for the past two years. I would also like to thank Dr. Richard Ash for helping me with the ICP-MS, and my fellow senior thesis students for offering their support, especially Justine Grabiec for working together with me in the clean lab and on the mass spectrometers. This work was made possible by support of the NSF Grant 1447174 to ISP; this support is greatly appreciated.

References

- Allègre C. J., Luck J. M. (1980) Osmium isotopes as petrogenic and geological tracers. *Earth and Planetary Science Letters* **48**, 148-154.
- Aitken B. G., Echeverria L. M. (1984) Petrology and geochemistry of komatiites and tholeiites from Gorgona Island, Colombia. *Contrib Mineral Petrol* **86**, 94-405.
- Alvarado G. E., Denyer P., Sinton C. W. (1997) The 89 Ma Tortugal komatiite suite, Costa Rica: Implications for a common geological origin of the Caribbean and Eastern Pacific region from a mantle plume. *Geology* **25**; no. 5, 439-442.
- Arndt N. T., Naldrett A. J., Pyke D. R. (1977) Komatiite and iron-rich tholeiitic lavas of Munro Township, Northeast Ontario. *Journal of Petrology* **18**, 319-369.
- Arndt N. T., Brooks C. (1980) Komatiites. *Geology* **8**, 155-156
- Arndt N. T. (1985) Differentiation of komatiites flows. *Journal of Petrology* **27**, 279-301.
- Arndt N. T., Kerr A. C., Tarney J. (1997) Dynamic melting in plume heads: the formation of Gorgona komatiites and basalts. *Earth and Planetary Science Letters* **146**, 289-301.
- Arndt N. T. (2003) Komatiites, kimberlites, and boninites. *Journal of Geophysical Research*. **108**.
- Arndt N. T., Leshner C. M., Barnes S. J. (2008) *Komatiite*. Cambridge University Press, Cambridge, UK.
- Barnes S. J., Naldrett A. J., Gorton M. P. (1985) The origin of the fractionation of platinum-group elements in terrestrial magmas. *Chem. Geol.* **53**, 303-323.
- Brandon A. D., Walker R. J., Puchtel I. S., Becker H., Humayun M., Revillon S. (2003) ^{186}Os - ^{187}Os systematics of Gorgona Island komatiites: implications for early growth of the inner core. *Earth and Planetary Science Letters* **206**, 411-426.
- Dupre B., Echeverria L. M. (1983) Pb isotopes of Gorgona Island (Colombia): isotopic variations correlated with magma type. *Earth and Planetary Science Letters* **67**, 186-190.
- Echeverria L. M. (1980) Tertiary or Mesozoic Komatiites from Gorgona Island, Colombia: Field Relations and Geochemistry. *Contrib. Mineral., Petrol.* **73**, 253-266.
- Echeverria L. M., Aitken B. G. (1986) Pyroclastic rocks: another manifestation of ultramafic volcanism on Gorgona Island, Colombia. *Contrib. Mineral Petrol.* **92**, 428-436.
- Gansser A. (1950) Geological and petrological notes on Geogona Island in relation to North-Western S America. *Schweiz Mineral Perogr Mitt* **30**, 219-237.
- Gansser A., Dietrich V. J., Cameron W. E. (1979) Paleogene komatiites from Gorgona Island. *Nature* **278**, 545-546.

- Kerr A. C., Marriner G. F., Arndt N. T., Tarney J., Nivia A., Saunders A. D., Duncan R. A. (1994) The petrogenesis of Gorgona komatiites, picrites and basalts: new field, petrographic and geochemical constraints. *Lithos* **37**, 245-260.
- Mertzman S. A. (2000) K–Ar results from the southern Oregon – northern California Cascade range. *Oregon Geol.* **62**(4), 99–122.
- Puchtel I.S., Touboul M., Blichert-Toft J., Walker R. J., Brandon A. D., Nicklas R. W., Kulikov V. S., Samsonov A. V. (2016) Lithophile and siderophile element systematics of Earth's mantle at the Archean Proterozoic boundary: Evidence from 2.4 Ga komatiites. *Geochim. Cosmochim. Acta* **180** 227-255.
- Puchtel I.S., Walker R.J., Brandon A.D., Nisbet E.G. (2009) Pt–Re–Os and Sm–Nd isotope and HSE and REE systematics of the 2.7 Ga Belingwe and Abitibi komatiites. *Geochim. Cosmochim. Acta* **73**, 6367-6389.
- Puchtel I. S., Brandon A. D., Humayun M., Walker, R.J. (2005) Evidence for the early differentiation of the core from Pt–Re–Os isotope systematics of 2.8-Ga komatiites. *Earth and Planetary Science Letters* **237**, 118-134.
- Pyke D. R., Naldrett A. J., Eckstrand O. R. (1973). Archean ultramafic flow in Munro Township, Ontario. *Geological Society of America Bulletin* **84**, 955-978.
- Trela J., Gazel, E., Sobolev A. V., Moore L., Bizimis M., Jicha B., Batanova V. G. (2017). The hottest lavas of the Phanerozoic and the survival of deep Archean reservoirs. *Nature Geoscience*. In press.
- Walker R. J., Storey M., Kerr A. C., Tarney J., Arndt N. T. (1999) Implications of ¹⁸⁷Os isotopic heterogeneities in a mantle plume: evidence from Gorgona Island and Curacao. *Geochim. Cosmochim. Acta* **63**, 713–728.
- Walker R. J., Echeverria L. M., Shirey S. B., Horan M. F. (1991) Re- Os isotopic constraints on the origin of volcanic rocks, Gorgona Island, Colombia: Os isotopic evidence for ancient heterogeneities in the mantle. *Contrib. Mineral Petrol.* **107**, 150-162
- Walker R. J., Carlson R. W., Shirey S. B., Boyd F. R. (1989) Os, Sr, Nd, and Pb isotope systematics of southern African peridotite xenoliths: Implications for the chemical evolution of subcontinental mantle. *Geochim. Cosmochim. Acta* **55**, 1583-1595.

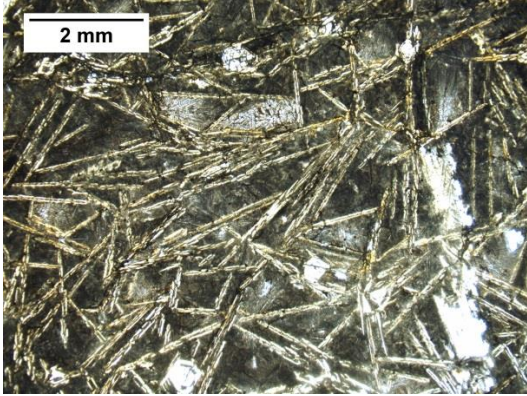
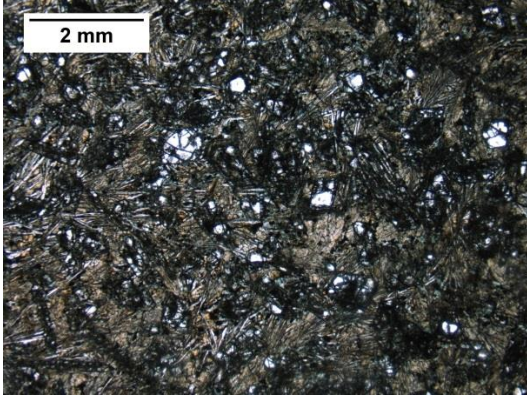
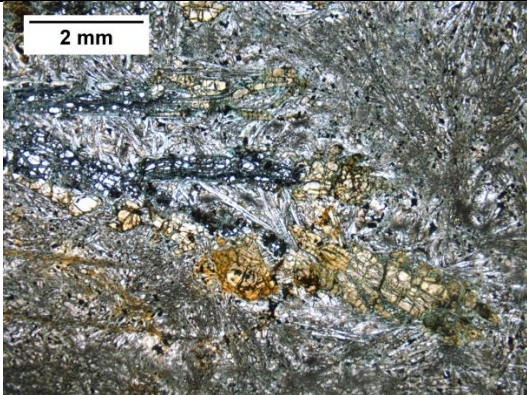
Appendix I

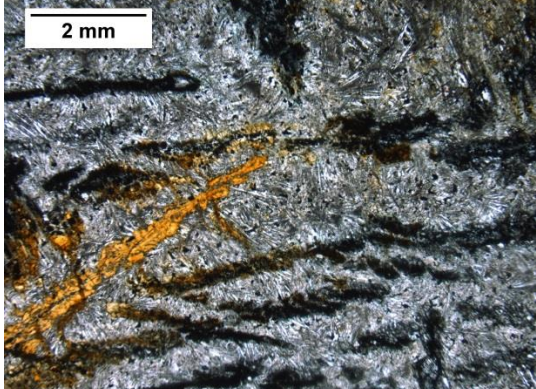
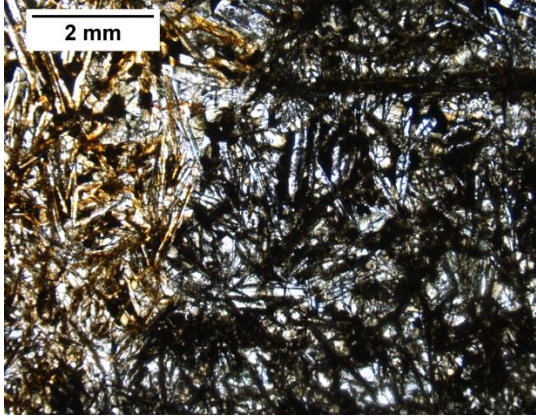
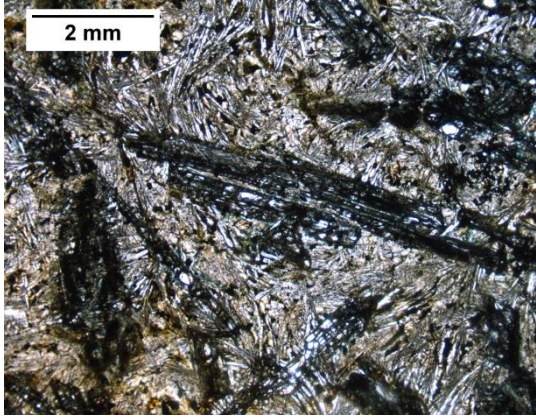
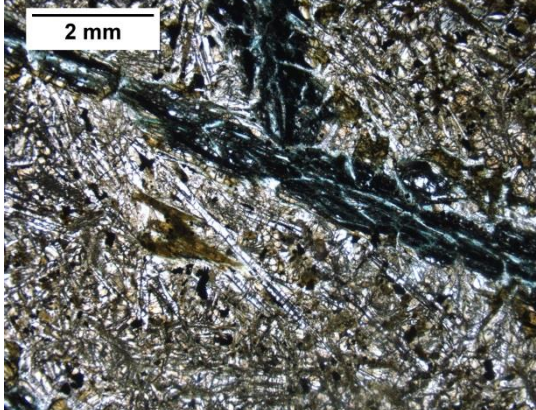
Major Element Chemistry

Sample	Lithology	SiO ₂	TiO ₂	Al ₂ O ₃	FeO	MnO	MgO	CaO	Na ₂ O	K ₂ O	P ₂ O ₅	Total
<i>Gorgona Island, East</i>												
GOR 152	komatiite	45.32	0.68	12.51	12.9	0.21	15.33	11.2	1.62	0.021	0.039	99.83
GOR 153	komatiite	44.12	0.51	9.67	12.22	0.2	23.8	8.22	0.93	0.005	0.032	99.707
GOR 155	komatiite	46.34	0.69	12.57	12.78	0.18	15.45	10.31	1.33	0.066	0.041	99.757
GOR 156	komatiite	44.98	0.63	11.79	12.68	0.21	17.65	10.25	1.27	0.021	0.038	99.519
GOR 157	komatiite	45.66	0.77	13.94	13.13	0.21	12.14	12.18	1.59	0.042	0.044	99.706
GOR 159	komatiite	44.51	0.61	11.57	12.75	0.21	18.77	9.81	1.23	0.02	0.036	99.511
GOR 160	komatiite	45.09	0.65	11.77	12.71	0.19	17.76	10.12	1.18	0.044	0.036	99.554
<i>Gorgona Island, West</i>												
GOR 23B	komatiite	44.7	0.67	12	12.5	0.19	18	9.97	0.92	0.03		98.98
GOR 47	komatiite	47.4	0.39	12.4	10.2	0.22	17.6	10.7	1.16	0.01		100.08
GOR 23A	basalt	52.7	1.83	12.8	13.4	0.21	5.25	9.13	2.61	0.14		98.07
<i>Tortugal Suite</i>												
TO-010513-5	picrite	46.05	0.59	5.58	10.88	0.18	30.58	5.34	0.26	0.03	0.19	100.26
TO-080514-2	picrite	46.44	0.91	4.60	10.92	0.17	32.22	5.32	0.14	0.19	0.20	101.74
TO-080614-5	picrite	47.50	0.59	5.61	9.96	0.17	31.45	5.05	0.15	0.10	0.19	101.39

Appendix II

GOR 152 – 160 flow photomicrographs

Photomicrograph (PPL) x1.5 magnification	Sample Number, Flow Position	Description
	GOR – 152 Upper chill margin (A ₁) Fig. 7	Large olivine spinifex phenocrysts throughout with a matrix of clinopyroxene and glass. Grains formed in situ. Lithology represents emplaced lava composition, as it was the first zone to crystalize. Also see skeletal spinifex – Fig. 2
	GOR – 153 Upper chill spinifex zone (A ₁₋₂) Fig. 8	Spinifex/upper chill zone. Micro spinifex is an indication of upper chilled margin.
	GOR – 155 Altered platy olivine spinifex (A ₂) Fig. 9	Small elongate, platy olivine spinifex. Beginning of true spinifex zone. Olivine in CPX and glass matrix.

	<p>GOR – 156</p> <p>Platy olivine spinifex (A₂)</p> <p>Fig. 10</p>	<p>Fine matrix of olivine spinifex with large elongate glass and OPX crystals.</p>
	<p>GOR – 157</p> <p>Platy olivine spinifex – evolved (A₂)</p> <p>Fig. 11</p>	<p>Matrix of olivine spinifex, opx and glass</p>
	<p>GOR – 159</p> <p>Platy olivine spinifex, with plagioclase – evolved (A₂)</p> <p>Fig. 12</p>	<p>Fine matrix of olivine spinifex and OPX with large elongate glass.</p>
	<p>GOR – 160</p> <p>Platy olivine spinifex, with plagioclase – evolved (A₂)</p> <p>Fig. 13</p>	<p>Fine matrix of olivine spinifex and OPX with large elongate glass and olivine.</p>

Appendix III

Honor Code:

"I pledge on my honor that I have not given or received any unauthorized assistance or plagiarized on this assignment."

Kyle Ludwig